Magnetization of granular high-T_c superconductors in strong magnetic fields

V. V. Val'kov and B. P. Khrustalev

L. V. Kirenskii Institute of Physics, Russian Academy of Sciences, Siberian Branch, 660036 Krasnoyarsk, Russia

(Submitted 11 August 1994; resubmitted 5 January 1995)
Zh. Éksp. Teor. Fiz. **107**, 1221–1231 (April 1995)

The remagnetization processes occurring in ceramic oxide superconductors in strong magnetic fields have been studied experimentally and theoretically. A model of the critical state, which makes it possible to take into account the granular structure of ceramic high-T_c superconductors, has been developed to interpret the experimental results. Equations describing the hysteresis loops of granular materials in strong magnetic fields have been derived for an arbitrary dependence of the critical current density on the magnetic induction. It has been established for the high-T_c superconductors investigated that the function $j_c(B)$ is characterized by the existence of two scaling parameters B_0 and B_1, which distinguish regions with different rates of decrease of j_c. The proposed form of $j_c(B)$ yields quantitative agreement between the experimental and theoretical hysteresis loops. The behavior of $j_c(B)$ thus obtained is in good agreement with that previously found in fields up to 5 kOe.

1. INTRODUCTION

It is known that high-temperature (high-T_c) superconductors are hard type-II superconductors.[1,2] Therefore, the magnetic and resistive properties of high-T_c superconductors are determined to a considerable extent by the distribution of the Abrikosov vortices throughout the volume of the material, as well as by the character of their pinning. One of the most important characteristics of high-T_c superconductors, the critical current density j_c, is related to the vortex structure and its degree of pinning. In single-crystal high-T_c superconductors the value of j_c is determined by the pinning force acting on the Abrikosov vortices. The investigation of j_c, particularly the determination of the dependence of j_c on the magnetic induction B, is of special importance, for example, from the viewpoint of studying specific mechanisms of vortex pinning and the possibility of regulating them with the aim of increasing the pinning force.

It should, however, be noted that the direct study of the characteristics of the transport current on the basis of an investigation of current-voltages characteristics is often associated with technical difficulties, which are due primarily to the formation of Ohmic contacts. For this reason, information on the critical current density is often obtained using so-called contactless methods. Among them the most important is the approach based on a study of the remagnetization of hard type-II superconductors in a slowly varying external magnetic field.[3]

When objects are selected to investigate the hysteresis curves of high-T_c superconductors, several circumstances must be taken into account. For example, when single-crystal high-T_c superconductors of cylindrical shape are employed in the simplest experimental geometry (with the field H parallel to the axis of the cylinder) and the radius of the cylinder is a macroscopic quantity ($R \sim 1-10^{-1}$ cm), the penetration field H_p can be so strong that the Abrikosov vortices effectively penetrate only into a thin surface layer. Therefore, only a small fraction of the superconducting material is probed. The situation is different for ceramic high-T_c superconductors, in which the superconducting regions are conglomerates of granules with a characteristic radius $R \sim 10^{-4}$ cm. The penetration field is significantly weaker for them, and the vortices can penetrate the entire depth of the granules.

The concept of a critical state is often utilized to describe the magnetic properties of type-II superconductors.[4–7] This approach provides a qualitatively correct description of the hysteresis loops even for polycrystalline high-T_c superconductors. However, the complex character of the magnetization processes in such superconductors requires that the granular state of the structure be considered in a quantitative treatment of experimental results. The granular structure has been taken into account in several investigations[3,8–12] in the region of the so-called low-field electrodynamics of high-T_c superconductors, but there have not been any theoretical papers which describe the hysteresis loops of high-T_c superconductors in strong ($H \sim 50$ kOe) magnetic fields and take into account the granular structure of the material.

This paper presents the results of a modified critical-state theory, which makes it possible to describe experimental hysteresis loops of polycrystalline high-T_c superconductors with consideration of their granular structure. The average over a statistical ensemble of granules is performed explicitly and equations which are convenient for calculating hysteresis curves are derived. A comparison of the calculated results with experimental hysteresis loops reveals good agreement. A new form of the dependence of the critical current density on the magnetic induction is proposed. The uniqueness of this dependence is characterized by the presence of two magnetic induction scales, which demarcate regions with different rates of decrease of the critical current density.

 1063-7761/95/040680-06$10.00

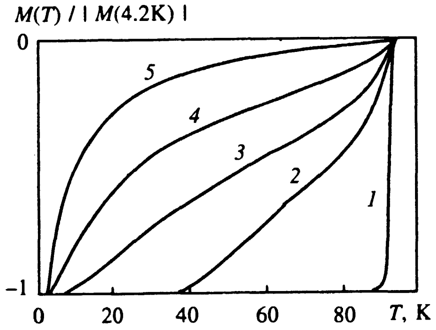

FIG. 1. Plots of the temperature dependence of the diamagnetic moment for various values of the magnetic field: *1)* $H=0.5$ Oe; *2)* $H=10$ Oe; *3)* $H=100$ Oe; *4)* $H=1$ kOe; *5)* $H=10$ kOe.

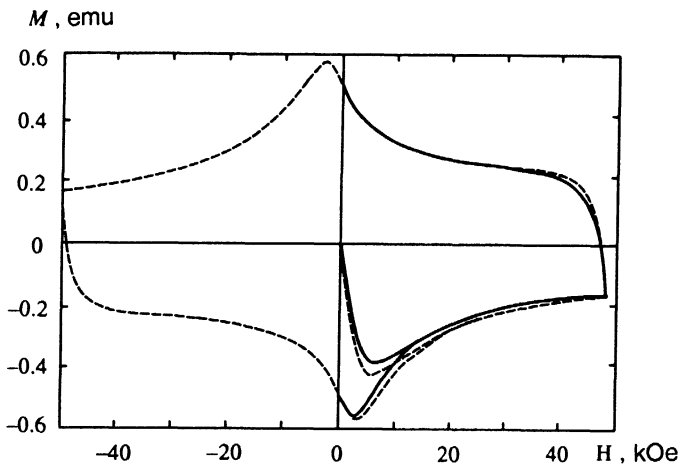

FIG. 2. Remagnetization hysteresis curve of a thallium ceramic (the mass of the sample was 85.5 mg). Dashed line—experiment. Solid line—theoretical curve.

2. EXPERIMENT

Y(123) ceramics prepared according to the "standard" technology,[13] as well as thallium ceramics modified by barium fluoride,[14] were investigated.

The measurements were performed on an automated vibrating magnetometer.[15] A compensation method for determining the magnetic moment was employed at $H>100$ Oe, and the measurements of j_c in weak fields were performed with direct amplification to eliminate the influence of the magnetic field of the compensation coil on the magnetic state of the sample.

Figure 1 presents plots of $M(T)$ at $H=$const for one of the Y(123) samples. The form of the curves is typical of all the ceramics investigated. The temperature of the transition to the superconducting state, which was determined from the appearance of a diamagnetic moment, coincides with the results of the determination of T_c from plots of the temperature dependence of the resistance of the sample. Although the external field has only a weak influence on the value of T_c, the character of the plot of $M(T)$ changes when even a comparatively weak field is applied, attesting to penetration of the field into intergranular regions. The plots of $M(T)$ and $M(H)$ measured in weak fields revealed that the effective value of H_{c1}, which is evidently determined by the properties of the "weak" intergranular regions, lies in the range from 1 to 10 Oe.

Figure 2 presents the hysteresis loops for a thallium ceramic. The form of each loop is typical of granular high-T_c superconductors, although the hysteresis loops for the samples of this series are more "open" than are the loops for Y(123) ceramics.

3. REMAGNETIZATION OF A GRANULAR STIFF SUPERCONDUCTOR

A complete description of the remagnetization processes in a granular stiff type-II superconductor can be obtained by using the model introduced in Ref. 9, which has been favorably endorsed for describing the low-field electrodynamics of ceramic high-T_c superconductors.[9,11,12] In our experiments the hysteresis loops were investigated mainly in fairly strong magnetic fields ($H<50$ kOe). At such values of H the weak links are completely broken, and the individual granules behave independently. The granular structure of the material is reflected in the need to average the remagnetization processes over a statistical ensemble of granules. The theoretical part of this paper is devoted to the solution of this problem.

The quantitative calculations of the magnetization curves were performed in the context of the doctrine known as the "critical state model." The dependence of the induction B on the radius r for an individual granule is specified by the equation[16]

$$\frac{dB(r)}{dr} \pm \frac{4\pi}{c} j_c(B). \tag{1}$$

It is convenient to represent the critical current in the form[17]

$$j_c(B)=j_c(0)/f(B), \tag{2}$$

where $j_c(0)$ is the critical current density when the induction vanishes and $f(B)$ is a nondecreasing function such that $f(B=0)=1$.

We characterize the statistical ensemble of granules by the function $\varphi(R)$, which is the distribution density of the superconducting granules with respect to the radius R. We use P to denote the fraction of the material which is concentrated in the superconducting granules. Then for a macroscopic ceramic sample of cylindrical shape with a radius R_0, the normalization condition has the form

$$P=\frac{1}{R_0^2}\int_0^\infty R^2\varphi(R)dR. \tag{3}$$

The definition of the magnetization readily yields a general equation for performing the calculations

$$4\pi M(H)=-H+(1-P)\mu_n H + \frac{2}{R_0^2}\int_0^\infty \varphi(R)\int_0^R rB(r)dr, \tag{4}$$

where μ_n is the magnetic permeability of the intergranular material. The specific form of the distribution of the magnetic induction $B(r)$ is determined by the magnetic field strength H, the radius of a granule R, and the history of the process. Therefore, expression (4) should be converted into a form which is convenient in practical work separately for the three cases.

3.1. The *ab* process

In this, the simplest, case the magnetic field H varies from zero to H_m, the sample being in the demagnetized state when $H=0$. At a fixed value of H the entire ensemble of granules naturally separates into two "subensembles." One of them includes the granules in which the vortices have penetrated through the entire depth of the granules. The other subensemble is clearly characterized by the fact that there is only partial penetration of the vortices through the granules. The quantitative characteristic which separates the two subensembles is R_H, which can be determined from the following equations

$$KR_H=\Phi(\mu_n H),\quad K=\frac{4\pi}{c}j_c(0),\quad \frac{d\Phi(B)}{dB}=f(B). \tag{5}$$

Physically, R_H is the radius of a granule for which the penetration field is equal to $\mu_n H$.

When the foregoing is taken into account and the notation introduced above is used, the general expression for the magnetization in the process under consideration can be represented in the form

$$4\pi M_{ab}(H)=(\mu_n-1)H-\left(\frac{1}{KR_0}\right)^2\int_0^{R_H}\varphi(R)dR \times\int_{B^+(H)}^{\mu_n H}[KR+\Phi(B)-\Phi(\mu_n H)]^2dB -\left(\frac{1}{KR_0}\right)^2\int_{R_H}^{\infty}\varphi(R)dR \times\int_0^{\mu_n(H)}[KR+\Phi(B)-\Phi(\mu_n H)]^2dB. \tag{6}$$

The value of $B^+(H)$ is numerically equal to the magnetic induction at the center of the granules with $R\leqslant R_H$, if the magnetic induction on the surface of granules at $r=R$ is equal to $\mu_n H$. The equation determining $B^+(H)$ has the form

$$\Phi\{B^+(H)\}+KR=\Phi(\mu_n H). \tag{7}$$

3.2. The *cd* process

The portion of the hysteresis loop from $H=H_m$ to $H=0$ (as the field H decreases) forms during this process. The appearance of a new value of H_m produces an additional characteristic radius R_m

$$KR_m=\Phi(\mu_n H_m). \tag{8}$$

The significance of this radius is that in the granules with $R<R_m$ there is a pinned flux throughout the entire volume of the granules, while in the granules with $R>R_m$ the Abrikosov vortices do not penetrate to the center of the granules. The appearance of dimensional scales specifying a division

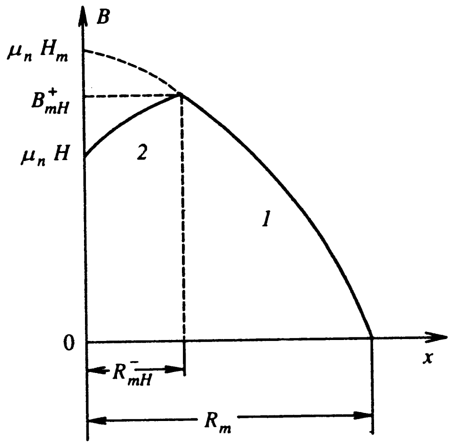

FIG. 3. Distribution of the magnetic induction and characteristic radii for the cd process.

of the statistical ensemble of granules into subensembles is shown in Fig. 3. If $H=H_m$ holds, $B(r)$ is described by curve *1* (the dashed portion is absent, as is curve *2*). When $H<H_m$ holds, the distribution of $B(r)$ is depicted by a broken curve composed of individual portions. The equations of these curves are clearly given by the following relations:

$$\Phi(B)-\Phi(\mu_n H_m)=-Kx, \tag{9}$$

$$\Phi(B)-\Phi(\mu_n H)=Kx, \tag{10}$$

where $x=R-r$ is the penetration depth. The new length scale appearing R^-_{mH} is defined in the following manner

$$R^-_{mH}=\frac{1}{2}(R_m-R_H). \tag{11}$$

Therefore, the statistical ensemble of granules naturally divides into three subensembles. The first subensemble contains the granules with $0\leqslant R\leqslant R^-_{mH}$. The granules in this subensemble have completed the transition process at a given value of H. The second subensemble contains granules with $R^-_{mH}\leqslant R\leqslant R_m$, which, as is seen from the diagram, are still undergoing the transition process. Finally, the granules of the third subensemble have radii $R>R_m$ and contain regions into which the Abrikosov vortices have not penetrated. Taking this into account, we have

$$4\pi M_{cd}(H)=(\mu_n-1) +\left(\frac{1}{KR_0}\right)^2\int_0^{R^-_{mH}}\varphi(R)dR\int_{\mu_n H}^{B^-(H)}[KR -\Phi(B)+\Phi(\mu_n H)]^2dB +\left(\frac{1}{KR_0}\right)^2\int_{R^-_{mH}}^{0}\varphi(R)dR\int_{\mu_n H}^{B^+_{mH}}[KR -\Phi(B)+\Phi(\mu_n H)]^2dB -\left(\frac{1}{KR_0}\right)^2\int_{R^-_{mH}}^{R_m}\varphi(R)dR\int_{B_m H}^{B^+_{mH}}[KR +\Phi(B)-\Phi(\mu_n H_m)]^2dB$$

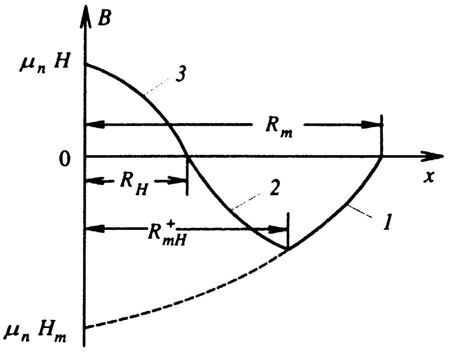

FIG. 4. Distribution of the magnetic induction and characteristic radii for the $a'b$ process.

$$-\left(\frac{1}{KR_0}\right)^2 \int_{R_m}^{\infty} \varphi(R)dR \int_0^{B^+_{mH}} [KR+\Phi(B) - \Phi(\mu_n H_m)]^2 dB. \tag{12}$$

The characteristic fields are determined from the solutions of the equations

$$\Phi[B-(H)]-KR=\Phi(\mu_n H),$$
$$2\Phi(B^+_{mH})=\Phi(\mu_m H_m)+\Phi(\mu_n H),$$
$$\Phi[B_m(0)]+KR=\Phi(\mu_n H_m). \tag{13}$$

It is obvious that the variation of H is accompanied by variation of the boundaries between the ensembles and by variation of the characteristic fields $B^-(H)$ and B^+_{mH}. Accordingly, it should be expected that when the ensemble of granules are dispersed sufficiently with respect to the radius, the granular structure of the high-T_c superconductor is capable of modeling the effect of an additional dependence of the critical current on the magnetic induction.

3.3. The $a'b$ process

The $a'b$ process refers to the formation of the portion of the hysteresis loop where the external magnetic field H increases from $H=0$ to $H=H_m$. The history for this process is defined by the "frozen" distribution of the induction formed when H decreased from $H=-H_m$ to $H=0$.

The systematic mathematical transition from Eq. (4) to convenient expressions is very cumbersome for the process under consideration. The final result can be graphically demonstrated with the aid of the diagram of the distribution of $B(r)$ presented in Fig. 4. The distribution of $B(r)$ for granules with $R>R_m$ is shown in the figure by the thick broken curve. The individual portions of this curve are described by the equations

$$\mathbf{1}:\quad \Phi(-B)-\Phi(\mu H_n)-Kx,\quad B\leqslant 0,\quad R^+_{mH}\leqslant x\leqslant R_m;$$
$$\mathbf{2}:\quad \Phi-(B)+\Phi(\mu_n H)=Kx,\quad B\leqslant 0,\quad R_H\leqslant x\leqslant R_{mH};$$
$$\mathbf{3}:\quad \Phi(B)-\Phi(\mu_n H)=-Kx,\quad B\geqslant 0,\quad 0\leqslant x\leqslant R_H. \tag{14}$$

It is seen that in this case an additional scaling radius R^+_{mH} appears along with the previously introduced scaling parameters R_m and R_H:

$$R^+_{mH}=\frac{1}{2}(R_m+R_H). \tag{15}$$

Clearly, the presence of three characteristic radii $R_m \geqslant R^+_{mH} \geqslant R^-_{mH}$ calls for the separation of the entire statistical ensemble of granules into four subensembles. After the corresponding transitions, the magnetization in the $a'b$ process can be represented in the form

$$4\pi M_{a'b}(H)=4\pi M_{ab}(H)-\sum_{i=1}^{4} I_i^{a'b}(H_m,H), \tag{16}$$

where $4\pi M_{ab}(H)$ is described by expression (6), and the terms in the sum have the form

$$I_1^{a'b}(H_m,H)=-\left(\frac{1}{KR_0}\right)^2 \int_{R_H}^{R^+_{mH}} \varphi(R)dR \int_0^{B_2^-(H)} [KR - \Phi(B)-\Phi(\mu_n H)]^2 dB,$$
$$I_2^{a'b}(H_m,H)=-\left(\frac{1}{KR_0}\right)^2 \int_{R^+_{mH}}^{\infty} \varphi(R)dR \int_0^{B^-_{mH}} [KR - \Phi(B)-\Phi(\mu_n H)]^2 dB,$$
$$I_3^{a'b}(H_m,H)=\left(\frac{1}{KR_0}\right)^2 \int_{R^+_{mH}}^{R_m} \varphi(R)dR \int_{B^+(H_m)}^{B^-_{mH}} [KR + \Phi(B)-\Phi(\mu_n H)]^2 dB,$$
$$I_4^{a'b}(H_m,H)=\left(\frac{1}{KR_0}\right)^2 \int_{R_{mH}}^{\infty} \varphi(R)dR \int_0^{B^-_{mH}} [KR+\Phi(B) - \Phi(\mu_n H_m)]^2 dB. \tag{17}$$

where the characteristic values of the magnetic induction satisfy the equations

$$\Phi[B_2^-(H)]-KR=-\Phi(\mu_n H),$$
$$2\Phi(B^-_{mH})=\Phi(\mu_n H_m)-\Phi(\mu_n H). \tag{18}$$

4. INTERPRETATION OF THE EXPERIMENTAL DATA

The specific calculations were performed using a statistical ensemble determined by the distribution function

$$\varphi(R)=N\frac{R}{\bar{R}}\exp\left\{-\left(\frac{R-\bar{R}}{\Delta}\right)^2\right\}. \tag{19}$$

The normalization constant is specified by the expression

$$N=\frac{P}{\Gamma(\delta)}\left(\frac{R_0}{\bar{R}}\right)^2\frac{1}{\bar{R}}. \tag{20}$$

The function $\Gamma(\delta)$ has the following integral representation

$$\Gamma(\delta)=\int_0^{\infty} y^3 \exp\left\{-\left(\frac{y-1}{\delta}\right)^2\right\}dy. \tag{21}$$

It is seen that in the limit $\Delta \ll \bar{R}$ the distribution function decays according to a Gaussian law for both $R > \bar{R}$ and $R < \bar{R}$. If the statistical ensemble of granules is characterized by a large spread, i.e., for $\bar{R} \sim \Delta$, the decrease in $\varphi(R)$ at small values of R is specified by the pre-exponential factor. Besides the distribution function of the statistical ensemble of granules, the dependence of the critical current density on the magnetic induction must be modeled. It should be noted that the frequently used Bean (j_c=const) and Kim–Anderson ($j_c \propto 1/B$) models do not provide good agreement between the experimental and theoretical hysteresis loops in our case. The dependence described by the expressions

$$j_c \propto \exp\left(-\frac{B}{B_0}\right), \quad j_c \propto \left(1+\frac{B}{B_0}\right)^{-1},$$

$$j_c \propto \left[1+\left(\frac{B}{B_0}\right)^2\right]^{-1}, \quad j_c \propto \ln^{-1}\left(e+\frac{B}{B_0}\right) \tag{22}$$

also proved to be unsatisfactory. A common difficulty was that if the experimental hysteresis loop was described well at low values of the external magnetic field ($H < 10$ kOe), there were large discrepancies at high values of H. On the other hand, if the flanks of the hysteresis curves were described well, significant discrepancies appeared at weak magnetic fields.

These difficulties could be overcome by selecting $j_c(B)$ in the following form:

$$j_c(B) = j_c(0)\left\{\frac{1-Qx}{1+x} + \left(\frac{B}{B_0}\right)^{\gamma}\right\}^{-1}, \tag{23}$$

where $x = B/B_1$. The main special feature of this dependence is as follows. The parameters having the dimensions of induction are B_0 and B_1. They determine the characteristic scales of the induction, which distinguish regions with qualitatively different variations of $j_c(B)$. For example, for $B_1 \ll B_0$ we have

$$j_c(B) = j_c(0)(1-x)/(1+Qx), \quad B \ll B_1$$

$$j_c(B) = j_c(0)[Q + (B/B_0)^{\gamma}]^{-1}, \quad B \gg B_1. \tag{24}$$

Thus, as B varies from zero to $B = B_1$, the current density decreases rapidly by a factor of Q. Then the rate of the drop in $j_c(B)$ decreases considerably, if $\gamma < 1$. The use of this two-scale parametrization for $j_c(B)$ made it possible to obtain calculated hysteresis loops which are in good agreement with the experimental loops. Here the function $\Phi(B)$ is defined by the expression

$$\Phi = QB + B_1(1-Q)\ln\left(1+\frac{B}{B_0}\right) + \frac{B_0}{1-\gamma}\left(\frac{B}{B_0}\right)^{1+\gamma}. \tag{25}$$

In Fig. 2 the solid lines show a hysteresis loop calculated using the present approach. The calculations were performed with parameters

$$B_0 = 2.5 \text{ kOe}, \quad B_1 = 0.8 \text{ kOe}, \quad Q = 5,$$

$$\gamma = 0.7, \quad \mu_n = 1.03. \tag{26}$$

The statistical ensemble of granules was characterized by the parameters

$$\Delta = 0.4\bar{R}, \quad K\bar{R} = 50 \text{ kOe}. \tag{27}$$

It is seen that the spread, which characterizes the dispersion of the values of the radii of the granules, is fairly high. If it is assumed that $R \cong 10$ μm and the spread has the value selected, the dimensions of the granules will fall in the range inferred from other experimental data.[3] Here the critical current density at a zero value of the induction has the value

$$j_c(0) = 3 \cdot 10^7 \text{ A/cm}^2, \tag{28}$$

which coincides with the characteristic value of j_c known for single-crystal high-T_c superconductors.

Using the values of the parameters in (26), we can analyze the behavior of $j_c(B)$ in our specific case. In the range of induction values from 0 to 5 kOe there is a sixfold decrease in j_c, and then there is a slow drop in the critical current density as the induction increases. This result correlates well with the conclusion in Ref. 18. In that paper the relation $j_c(B) = j_c(0) \cdot \exp(-B/B_1)$ was used to treat data on the critical current in $YBa_2Cu_3O_{7-\delta}$. Good agreement was obtained when the hysteresis loops in fields up to 5 kOe were studied, assuming $B_1 = 1$ kOe. In this context we recall that in our work the corresponding scaling parameter is equal to 0.8 kOe. In addition, it was established in the paper just cited that $j_c(0) = 2 \times 10^7$ A/cm^2. We found $j_c(0) = 3 \times 10^7$ A/cm^2 at $B = 0$ for our own sample. We note one more point of concurrence. Ravikumar and Chaddah[18] observed that j_c decreased by approximately a factor of three at $B_1 = 1$ kOe. A similar decrease in j_c occurred in the superconductors which we investigated at $B \cong B_1$. On the other hand, it should be noted that exponential decay of the critical current density cannot occur when $B \gg B_1$. To obtain the correct value of j_c for $B \gg B_1$, the law governing the variation of j_c must be different. This circumstance was taken into account in our proposed dependence of the critical current density on the magnetic induction.

5. CONCLUSIONS

Our modification of the model of the critical state made it possible to include the granular structure of ceramic high-T_c superconductors. The statistical dispersion of the dimensions of the individual granules was modeled by introducing an ensemble of noninteracting granules. The justification for this is that the hysteresis loops were investigated in relatively strong magnetic fields. The equations presented in this paper for the magnetization are applicable to an arbitrary form of $j_c(B)$. This permits their use to regenerate the critical current density at large values of B, at which $j_c(B)$ can have a complex character. The final expressions describing the individual portions of the hysteresis loop contain characteristics of the superconducting material of the granules, the magnetic permeability of the intergranular matter, and the volume fraction of the superconducting granules in the sample. Taken together, they permit application of the approach developed to the study of the magnetic properties of single-crystal high-T_c superconductors with the use of ceramic superconductors in the experiment. This proposition was demonstrated above in the determination of $j_c(B)$.

[1] J. G. Bednors and K. A. Müller, Z. Phys. B **64**, 189 (1986).
[2] L. P. Gor'kov and N. B. Kopnin, Usp. Fiz. Nauk **56**, 117 (1988) [Sov. Phys. Usp. **31**, 850 (1988)].
[3] E. Z. Meĭlikov, in *Reviews of High-T_c Superconductors* [in Russian], 1990, No. 1, p. 81.
[4] C. P. Bean, Phys. Rev. Lett. **8**, 250 (1962).
[5] Y. B. Kim, C. F. Hempstead, and A. R. Strnad, Phys. Rev. **129**, 528 (1963).
[6] H. London, Phys. Lett. **6**, 162 (1963).
[7] P. W. Anderson and Y. B. Kim, Rev. Mod. Phys. **36**, 39 (1964).
[8] H. Dersch and G. Blatter, Phys. Rev. B **38**, 11391 (1988).
[9] K.-H. Müller, Physica C (Amsterdam) **159**, 717 (1989).
[10] S. L. Ginzburg, G. Yu. Logvinova, I. D. Luzyanin *et al.*, Zh. Éksp. Teor. Fiz. **100**, 532 (1991) [Sov. Phys. JETP **73**, 292 (1991)].
[11] K.-H. Müller, D. N. Matthews, and R. Driver, Physica C (Amsterdam) **191**, 339 (1992).
[12] K.-H. Müller, in *Magnetic Susceptibility of Superconductors and Other Spin Systems*, edited by R. A. Hein, T. L. Francavilla, and D. H. Liebenberg, Plenum, New York, 1991.
[13] C. W. Chu, P. H. Hor, R. L. Meng *et al.*, Phys. Rev. Lett. **58**, 405 (1987).
[14] V. E. Volkov, A. D. Vasil'ev, Yu. G. Kovalev *et al.*, Pis'ma Zh. Éksp. Teor. Fiz. **55**, 591 (1992) [JETP Lett. **55**, 616 (1992)].
[15] A. D. Balaev, Yu. V. Boyarshinov, M. M. Karpenko, and B. P. Khrustalev, Prib. Tekh. Éksp. **3**, 165 (1985).
[16] P. G. de Gennes, *Superconductivity of Metals and Alloys*, W. A. Benjamin, New York-Amsterdam (1966) (Russ. transl. Mir, Moscow, 1968, p. 280).
[17] M. Forsthuber and G. Hilscher, Phys. Rev. B **45**, 7996 (1992).
[18] G. Ravi Kumar and P. Chaddah, J. Supercond. **2**, 247 (1989).

Translated by P. Shelnitz